Response to CO_2 doubling of the Atlantic Hurricane Main Development Region in a High-Resolution Climate Model

Takeshi Doi[1, 2], Gabriel A. Vecchi[2], Anthony J. Rosati[2], and Thomas L. Delworth[2]

1 Atmospheric and Oceanic Sciences Program, Princeton University, Princeton, NJ, U.S.A.

2 NOAA/Geophysical Fluid Dynamics Laboratory, Princeton, NJ, U.S.A.

J. Climate

(in press)

Corresponding author address: Takeshi Doi, Geophysical Fluid Dynamics Laboratory/NOAA, Princeton University Forrestal Campus, 201 Forrestal Road, Princeton, NJ 08542, USA, Tel: +1-609-452-6511, Email: Takeshi.Doi@noaa.gov

(Current affiliation: Japan Agency for Marine-Earth Science and Technology (JAMSTEC), 3173-25 Showa-machi, Kanazawa-ku,Yokohama, 236-0001, Japan Tel: +81-45-778-5512, Email: takeshi.doi@jamstec.go.jp)

Abstract

Response of climate conditions in the Atlantic Hurricane Main Development Region (MDR) to doubling of atmospheric CO_2 has been explored, using the new high-resolution coupled Climate Model version 2.5 developed at the Geophysical Fluid Dynamics Laboratory (GFDL-CM2.5). In the annual mean, the SST in the MDR warms by about 2°C in the CO_2 doubling run relative to the Control run, the trade winds become weaker in the northern tropical Atlantic, and the rainfall increases over the ITCZ and its northern region. The amplitude of the annual cycle of the SST over the MDR is not significantly changed by CO_2 doubling. However, we find that the interannual variations show significant responses to CO_2 doubling: the seasonal maximum peak of the interannual variations of the SST over the MDR is about 25% stronger than in the Control run. The enhancement of the interannual variations of the SST in the MDR is due to changes in effectiveness of the Wind-Evaporation-SST (WES) positive feedback: WES remains a positive feedback until boreal early summer in the CO_2 doubling run. The enhancement of the interannual variability of the SST over the MDR in boreal early summer due to CO_2 doubling could lead to serious damages associated with the Atlantic Hurricane count and drought (or flood) in the Sahel and South America in a future climate.

1. Introduction

Future climate response of the northern tropical Atlantic SST is a topic of substantial research, in part because of its potential impact on regional extreme events. Recent studies suggest that the Atlantic Hurricane activity may be modified in a future climate due in part to warmer SST anomalies in the northern tropical Atlantic, although there are uncertainties to the sign and magnitude of the change (Emanuel 2005; Swanson 2008; Vecchi et al. 2008; Knutson et al. 2010; Villanini et al. 2011). Also, climate changes in the northern tropical Atlantic SST influence rainfall over South America and the Sahel region through the meridional migration of the ITCZ and the West African Monsoon (Chiang et al. 2003; Kusnhir et al. 2005; Hagos and Cook 2008; Biasutti and Sobel 2009). Held et al. (2005) suggested that an observed drying trend in the Sahel may be due to both increased aerosol loading and increased greenhouse gases, although there remains some uncertainty regarding the response of the Sahel rainfall to greenhouse gases (Cook et al 2008). Interestingly, impacts of Atlantic variations are not restricted to the Atlantic Basin and can reach far to the Indian Ocean, the global Northern Hemisphere, and global climate (Zhang and Delworth 2006; Lu et al. 2006; Zhang et al. 2007; Sutton and Hodson 2005; 2007; Kucharski et al. 2008; Ding et al. 2011). Recently, Kucharski et al. (2011) suggested that the Atlantic warming in the 20th century might have reduced the Pacific warming through modifications of the Walker circulation using regionally coupled models.

Most previous work has mainly focused on response of the annual mean of the northern tropical Atlantic SST to a future climate and relatively less attention has been paid to response of the interannual variations to radiative forcing changes. The interannual variations of the northern tropical Atlantic SST are strongly phase-locked to the annual cycle, which is referred to as "seasonal phase-locking": the standard deviation of the SST develops from early boreal winter, reachs a maximum in boreal spring, and decays abruptly in boreal summer (Enfield and Mayer 1997; Doi et al. 2010). Reasonable simulation of this seasonal dependence in a climate model is critical for seasonal prediction of the Tropical Atlantic Variability, which can influence prediction of the year-to-year variations of the Atlantic Hurricane and drought (or flood) in the Sahel and South America (e.g. Zhao et al. 2009; 2010; Vecchi et al. 2011; Chen and Lin 2012). Therefore, in this manuscript, we explore future climate response of the seasonal phase-locking of the interannual variations of the northern tropical Atlantic SST.

In order to assess response of climate changes, it is desirable to use a model that reproduces the characteristic of observed variability. Therefore, for this study, we used present-day Control and CO_2 doubling runs with a new high-resolution fully atmosphere-ocean coupled general circulation model described in Delworth et al (2012); Climate Model version 2.5 developed at the Geophysical Fluid Dynamics Laboratory (GFDL-CM2.5). This model shows relatively high performance in simulating the tropical Atlantic. Improvements in the simulation of the ITCZ merdional migration allow for better

representation of the air-sea coupled processes in CM2.5 that are important for an abrupt seasonally phase-locked decay of the interannual SST anomaly in the northern tropical Atlantic (Doi et al. 2012). As the model biases in the tropical Atlantic variability with CM2.5 have been discussed carefully in Doi et al (2012), we would like to focus on the CO_2 doubling response in this paper. A brief description of the high-resolution CM2.5 modeling system and the experiments analyzed here is given in section 2. Using outputs from these experiments, we explored response to CO_2 doubling of the SST over the Atlantic Hurricane Main Development Region (MDR: 80°-20°W, 10°-25°N), which is referred to as the SST_{MDR}. The SST_{MDR} is used as the local positive correlated climate predictor for the Atlantic Hurricane statistical-dynamical prediction model developed by Vecchi et al (2011) and Villarini et al. (2011), the other negative correlated predictor for the Atlantic Hurricane being SST averaged in global tropics. The SST_{MDR} is thus an important quantity to represent realistically in models and predict its further evolution. Changes of the annual mean and the annual cycle of the SST_{MDR} are discussed in sections 3a and b. Response of the interannual variations of the SST_{MDR} is discussed in section 3c. The final section presents a summary and discussion of the results.

2. Model (GFDL-CM2.5)

GFDL-CM2.5 (Delworth et al. 2012; Doi et al. 2012) is a new high-resolution

model version that derives closely from GFDL-CM2.1 (Delworth et al. 2006, Gnanadesikan et al. 2006, Stouffer et al. 2006, and Wittenberg et al. 2006). The oceanic component of CM2.5 uses a 0.25° horizontal resolution of MOM4p1 in the tropics with the z* vertical coordinate (Griffies 2010; Griffies et al. 2012), which varies from 28km near the tropics to 8km in polar regions. It has a similar oceanic component to that of the CM2.4 model of Farneti et al. (2010). It is coupled to a 50km horizontal resolution atmosphere model with 32 vertical levels on a cubed-sphere grid (Lin 2004; Putman and Lin 2007). This formulation avoids the numerical problem of the convergence of meridians at the poles and allows grid boxes of roughly equal area over the globe. No flux adjustments are employed. The ocean model does not contain a parameterization for mesoscale eddy mixing. The land model is LM3 (Shevliakova et al. 2009; Milly et al. *in preparation*), which represents snow and rain interception on vegetation, as well as water phase change in the soil and snow pack. CM2.5 is initialized and forced in similar fashion to CM2.1 (Delworth et al. 2012; Delworth et al. 2006); the oceanic initial condition is taken from the end of one-year spin-up from observed climatological conditions at rest and the atmospheric initial condition is taken from the end of a simulation with prescribed SSTs.

We used monthly mean outputs from a 280 year simulation of CM2.5 with 1990 radiative forcing as the Control run. The idealized climate change response run is conducted from the present-day Control integration. The CO_2 doubling ($2 \times CO_2$) experiment of GFDL-CM2.5 is performed for 140 years following the framework described

in Delworth et al 2012; the model is forced with a 1% per year increase in atmospheric CO_2 concentration from year 101 of the 1990 Control simulation and reaches CO_2 doubling after 70 years. After that, the CO_2 concentration is held fixed at twice its present-day Control value and the integration continues thereafter. In this paper, model year 1 is defined as a year when the CO_2 doubling run starts.

3. Results

a. Annual mean

We begin by exploring time series of the SST_{MDR} in model year 1-140 of the Control and the CO_2 doubling runs (Fig. 1). In this paper, we focus on the model outputs after CO_2 stabilization because we are interested in equilibrium response and assessment of changes in variability through the transient forcing phase is not straightforward. As indicated in Fig.1, we can assume and discuss response of steady state to CO_2 doubling in years 91-140, although there is a weak upward trend in the CO2 doubling run. We thus calculate monthly climatologies by averaging monthly mean output for years 91-140.

In years 91-140, the annual mean SST_{MDR} in the $2\times CO_2$ experiment (26.9°C) warms by about 2°C relative to the Control run (25.0°C), which is colder by 1.3 °C relative to observatioal esitamte of the HadISST data averaged in 1960-2009 (26.3°C). The reader

is referred to Doi et al (2012) for a more discussion of the tropical Atlantic biases from observations in this model. Although the warm SST bias in the eastern equatorial region and the cold SST bias in the eastern MDR still remains in CM2.5 (Fig. 1 in Doi et al 2012), CM2.5 successfully improved simulations of seasonal-interannual variations of the northern tropical Atlantic SST and precipitation through better representation of the ITCZ migration. This is a good advantege to use CM2.5 for this study,

Figure 2 shows response to CO_2 doubling of the annual mean surface climate in the tropical Atlantic, along with the mean state of the Control run. The warming of SST in the Northern Hemisphere due to CO_2 doubling is about 0.2°C larger than that in the Southern Hemisphere (Fig. 2b). This meridional gradient of the response to CO_2 doubling of SST has an associated northward migration of the Atlantic ITCZ (Fig. 2d), which results in southwesterly wind anomalies and thus weaker trade winds in 5°-20°N (Fig. 2f). We found 20% more rainfall over the ITCZ and its northern region, while 20% less rainfall over the southern region of the ITCZ and South America. The hemispheric asymmetric response of the annual mean SST, precipitation, and wind fields to CO_2 doubling in CM2.5 is consistent with the climate change response of the annual mean fields across other climate models shown in Xie et al. (2011). They showed that a greater warming in the Northern Hemisphere than in the Southern Hemisphere is accorded with asymmetries in trade wind changes. However, they focused on the annual mean fields changes and did not examine response of seasonal and interannual variations to CO_2 doubling, which will be

shed light on in next subsections.

b. Mean seasonal cycle

The Control run with CM2.5 can reasonablely capture the seasonal cycle of SST_{MDR}, although the warming tendency in April-June was delayed by one month and the maximim peak in September is 30% larger relative to observation (Fig. 3). It is plausible to expect that the significant changes of the annual mean fields due to CO_2 doubling could connect to changes in the mean seasonal cycle. However, analysis of response of the seasonal variation of the surface climate in the MDR to CO_2 doubling does not indicate any substantial changes in this model. For example, the difference of the amplitude of the seasonal cycle of the SST_{MDR} between the Control run and the CO_2 doubling run is small and not significant, which is less than 5% of the amplitude of the seasonal cycle in the Control run.

Although significant changes in the seasonal cycle are not identified, it is possible that the magnitude and the seasonal phase-locking of the interannual variability may change in response to CO_2 doubling. We explore this possibility in next subsection.

c. Interannual variations

To assess interannual variability, we define anomaly fields as deviations from the monthly mean climatology. We remove the decadal variability using an eight-year running mean filter on a basis of spectrum analysis, because we focus on the interannual variation of the SST_{MDR} rather than its decadal variability. Fig. 4 shows the time series of the monthly SST_{MDR} anomalies and their probality density funcitions. We can find that the number of warm month beyond 0.6ºC increases in the 50 years relative to the Control run. This feature is more clarified by the monthly standard deviations of the interannual anomalies of the SST_{MDR} (Fig. 5). The Control run with CM2.5 can reasonably capture the seasonal phase-locking of the standard deviation of the SST_{MDR} in observation: the SST_{MDR} variance develops from early boreal winter, reachs a maximum in boreal spring, and decays abruptly in boreal summer, although the standard deviation in boreal spring-fall in the Control run is overestimated relative to the recent 50-years observarion (Fig. 5b). This model bias is mainly due to the western region of MDR, where the variabiliby is strongly influenced by the complicated topography and oceanic eddy activity. Doi et al (2012) showed that the interannual variation over the western region of MDR is highly simulated with CM2.5.

Interestingly, we find that the maximum peak in variability in the CO_2 doubling run appears in May, which is two months later than that in the Control run (Fig. 5a). The maximum difference in interannual variability between the CO_2 doubling run and the Control run appears in May-July. The interannual variation of the SST_{MDR} in May-July is 25% stronger in the CO_2 doubling run relative to the Control run. F-test of the ratio of

variances established the 95% statistical significance of the difference between the standard deviations of the two runs in May-July. The separation of $2\times CO_2$ response of the other 50-years mean standard deviations from the full years of the Control run suggests that the enhancement of the interannual variations due to CO_2 doubling during early boreal summer is robust relative to the natural variability exhibited by the available Control run outputs, although the Control run varies to some extent. The natural variability of the interannual variations of the SST_{MDR} in the Control run is very interesting, but it is beyond the scope of this paper. The two month shift in the maximim peak due to CO_2 doubling might be a part of the natural variability (Fig. 5a). Threfore, the enhancement of the interannual variations due to CO_2 doubling during early boreal summer is the focus in this manuscript. Note that we also investigated the CO_2 doubling response of GFDL-CM2.1 for 300-year integration. We compared the last 100 years of the CO_2 doubling experiment with the pre-industrial Control run with CM2.1. That also shows the 40% enhancement of the year-to-year SST variation over the MDR in May-July due to CO2 doubling. This result could support our results with CM2.5 although CM2.1 has a bias of boreal summer decay of year-to-year SST variation over the MDR (Doi et al. 2012).

We explore a composite analysis to help understanding the mechanism of the response to CO_2 doubling of the interannual variations of the SST_{MDR}. We construct a composite by averaging, based on selecting warm SST_{MDR} years, when the SST_{MDR} anomaly exceeds one standard deviation in month of the maximum peak. The details are shown in

Table 1.

In the warm SST_{MDR} year composite, the SST_{MDR} anomaly in the Control run is 0.42ºC in the maximum peak month of March-May, while the SST_{MDR} anomaly in the CO_2 doubling run is 0.55ºC in the maximum peak month of May-July. The maximum difference in the SST_{MDR} anomaly between the Control run and the CO_2 doubling run is found in May-July, when the SST_{MDR} anomaly warms by about 0.2°C in the CO_2 doubling run relative to the Control run (Fig. 6). The warm SST_{MDR} anomaly in the CO_2 doubling run is significantly enhanced by 60% in May-July relative to the Control run.

Interestingly, observations indicate that such an enhancement of interannual variability may be present in the historical record (Fig. 5b and 6a). The Hadley Center SST (HadISST; Rayner et al. 2003) and the Extended Reconstructed SST version 3 (ERSSTv3b; Smith et al. 2008) shows 10-25% enhancement of interannual SST_{MDR} variability in April-June in a warmer climate of the recent 50 years (1960-2009) relative to the early 50 years (1881-1930) (Fig. 5b). Also, the warm SST_{MDR} years composite field from the HadISST data shows that the SST_{MDR} anomaly is warmer by about 0.15°C in a warmer climate of the recent 50 years relative to the early 50 years (Fig. 6a). However, the extent to which this observed change is due to radiative forcing or internal variability remains to be determined.

To explore the mechanism behind the change in interannual variability, we calculated the diagnostic bulk mixed-layer heat budget over the MDR;

$$\frac{\partial T_{mix}}{\partial t} = \frac{Q - q_{sw}}{\rho C_p H_{mix}} + ocean\ dynamics\ contribution \quad . \qquad (1)$$

Here, T_{mix} is the mixed-layer temperature, a proxy for SST, ρ is the typical sea water density (1025 kg m^{-3}), C_p is the typical heat capacity of the sea water (3996 J kg^{-1} K^{-1}), and H_{mix} is the mixed-layer depth, which is calculated monthly as the depth at which the potential density becomes 0.125 kg m^{-3} larger than the surface density, as used by Levitus (1982). The quantity Q denotes the net surface enthalpy flux (including shortwave radiation, longwave radiation, latent heat flux, and sensible heat flux), and q_{sw} is the downward solar insolation that penetrates below the bottom of the mixed-layer. Thus, the first term on the right hand side, $\frac{Q - q_{sw}}{\rho C_p H_{mix}}$, represents the influence of net energy flux on the mixed-layer heat budget, which is referred as "the surface enthalpy flux contribution" hereafter. Note that "the surface enthalpy flux contribution" is different from Q: "the net surface enthalpy flux". The ocean dynamical contribution is simply estimated by difference between rate of change of the mixed-layer temperature and the surface enthalpy flux contribution.

In the Control run, the warming tendency of the SST_{MDR} during boreal spring is mainly due to the surface enthalpy flux contribution until April, when the warm SST_{MDR} starts to decay (Fig. 7a). Meanwhile, in the CO_2 doubling run, the warm SST_{MDR} anomalies still keep warming until June (Figs. 7b). The maximum difference of the warming tendency between the Control run and the CO_2 doubling run is found in May, arising mainly from differences in the surface enthalpy flux contribution (Fig. 7c). We note that interannual

variations of surface enthalpy flux contribution, $\frac{Q-q_{sw}}{\rho C_p H_{mix}}$ in Eq. 1, includes not only interannual variations of surface enthalpy flux, but also interannual variations of mixed-layer depth. However, we have confirmed that interannual variations of mixed-layer depth do not contribute to the differences in the surface enthalpy flux contribution over the MDR in boreal spring-summer (figure not shown).

The surface enthalpy flux anomalies, i.e. the Q anomalies, from boreal winter through boreal spring are dominated by wind-induced latent heat flux anomalies in the Control run and the CO_2 doubling run (Figs. 7d and e). It suggests that the Wind-Evaporation SST (WES) positive feedback (Xie 1999) develops the warm SST anomalies over the northern tropical Atlantic similarly both in the Control run and the CO_2 doubling run; the WES positive feedback is associated with the meridional migration of the ITCZ: 1) an anomalously northward migration of the ITCZ causes southwesterly wind anomalies in the northern tropics leading to weaker trade winds, 2) this results in less evaporation and thus suppressed latent heat loss from ocean, leading to warmer SST in the northern tropical Atlantic. 3) The outcome is the further northward migration of the ITCZ. The dominance of this mechanism in the growth of anomalies has been discussed in previous work (Carton et al. 1996; Chang et al. 1997; Xie 1999; Mahajan et al. 2010). Also, Doi et al. (2012) show that the WES feedback is reasonably captured in the Control run of CM2.5.

The siginificant difference in the surface enthalpy flux anomalies between the

Control run and the CO_2 doubling run is found in May, which is due to latent heat flux, primarily the wind-induced component (Figs. 7c and f). We also note the shortwave contribution in May, although it does not show principal difference between the Control run and the CO_2 doubling run. In the Control run, both latent heat and shortwave radiative flux anomalies are important for driving the cooling tendency in May (Fig. 7d). The shortwave cooling arises mainly from increased cloud amount tied to the enhanced convection that follows the warm SST anomalies. In the CO_2 doubling run, the shortwave radiation anomalies are very similar to those in the Control run.

The difference in wind-induced latent heat flux anomalies between the Control run and the CO_2 doubling run can be written as ($\left.\frac{\partial Q_{LH}}{\partial W}\right|_{CO_2} W'_{CO_2} - \left.\frac{\partial Q_{LH}}{\partial W}\right|_{CTL} W'_{CTL}$), where Q_{LH} is latent heat flux, W'_{CO_2} and W'_{CTL} is the composite anomaly of the surface wind speed in the CO_2 doubling run and the Control run respectively. $\frac{\partial Q_{LH}}{\partial W}$ is simply estimated by the climatology of lantent heat flux diveded by the climatology of surfae wind speed. Figure 8 shows the difference in wind-induced latent heat flux anomalies and wind stress anomalies during April-June between the CO_2 doubling run and the Control run. It is suggested that the positive WES feedback has already ended in the Control run by April, while the WES feedback keeps warming SST_{MDR} through June in the CO_2 doubling run (Figs. 7d,e,f). In May, the weak anomalies of the trade winds are larger in the CO_2 doubling run than those in the Control run (Fig. 8b), which enhance the suppressing of latent heat loss from ocean

in the CO_2 doubling run (Fig. 8a).

We assume linear relation between the interannual anomalies of wind speed and those of SST over the MDR $(W' \approx \alpha SST')$ and calculated the least squares estimate of the slope of this linear relation in model years 91-140. The slope in the CO_2 doubling run in boreal spring is -0.80 m s^{-1} per °C, which is similar to -0.83 m s^{-1} per °C in the Control run. A negative value shows that warm SST anomalies are associated with weak wind speed anomalies, which suggests the WES coupling. In boreal summer, the slope in the CO_2 doubling run is -0.37 m s^{-1} per °C, which is about twice of -0.17 m s^{-1} per °C in the Control run. It shows that the coupling between the SST variations and the wind speed variations is stronger in the CO_2 doubling run in boreal summer relative to the Control run. Therefore, we can conclude that there is an associated increase in the interannual variability of winds and wind-induced latent heat fluxes due to CO_2 doubling, much likes the SST. Note that the cold SST_{MDR} years can be explained by using similar mechanisms of opposite sign to the warm years (figures not shown)

Finally in this section, we estimate likely impacts on the Atlantic Hurricane activity and the rainfall field by the change in the characteristic of the interannual variability over the MDR. Table 2 gives Atlantic Hurricane counts estimated by the Atlantic Hurricane statistical-dynamical prediction model developed by Vecchi et al (2011), using the methodology of Villarini et al. (2011; 2012). This Atlantic hurricane model is based on the Poisson regression model in which the rate of occurrence is a linear function

of two climate predictors: the SST_{MDR} and SST averaged over the global tropics. Mean Atlantic Hurricane count decreases by 10% in the CO_2 doubling run relative to the Control run. In warm SST_{MDR} year composite, the Atlantic Hurricane count increases in observation, which is also consistent with Kossin and Vimont (2007). The Control run shows that the Atlantic Hurricane count significantly increases by about 30% in warm SST_{MDR} year relative to the mean count, while the CO_2 doubling run shows that the Hurricane count significantly increases in warm SST_{MDR} year by about 45% relative to the mean count. Interestingly, the increase of Hurricane count in warm SST_{MDR} years is enhanced by 20% in the CO_2 doubling run relative to the Control run, even though the mean count shows reduction in the CO_2 doubling run. This enhancement of the interannual variation of Atlantic Hurricane count is consistent with the large interannual variability of the SST_{MDR} in boreal early summer in the CO_2 doubling run. Also, the warm SST_{MDR} anomalies in boreal early summer in the CO_2 doubling run are associated with the northward migration of the ITCZ: more rainfall over 5°-10°N and less rainfall over 5°N-5°S and South America (Fig. 6c).

4. Summary and discussions

Using outputs from present-day Control and CO_2 doubling runs with the new high-resolution fully coupled GCM (GFDL-CM2.5), response of SST over the Atlantic

hurricane Main Development Region (SST_{MDR}) to CO_2 doubling has been investigated. The annual mean SST_{MDR} increases by about 2°C in the CO_2 doubling run relative to the Control run and by about 0.3°C more than the southern tropical Atlantic. The warmer SST_{MDR} drives a northward migration of the Atlantic ITCZ, which causes southwesterly wind anomalies and thus weaker trade winds in the northern tropical Atlantic. The SST, wind, and precipitation changes seem to develop in a positive WES feedback. This is consistent with Xie et al. (2011), who discussed that latent heat flux are important for the climate change pattern of the annual mean SST via the WES feedback.

The amplitude of the annual cycle of the SST_{MDR} is not significantly changed due to CO_2 doubling. However, we find a significant change of the interannual variations: the maximum peak of the interannual variations of the SST_{MDR} in the CO_2 doubling run moves from boreal spring to early boreal summer, at which time it is about 25% stronger relative to the Control run. Although the shift in the maximim peak due to CO_2 doubling might be the natural variability, the enhancement of the interannual variations due to CO_2 doubling during early boreal summer is robust and statistically significant in these two runs. The enhancement of the interannual variation of SST_{MDR} in boreal early summer also seems to appear in the observation, although there are some uncertainties among observational datasets. The large interannual variations of the SST_{MDR} during early boreal summer in the CO_2 doubling run is due to changes in the effectiveness of the WES positive feedback in a warmer climate: WES remains a positive feedback until early boreal summer in the CO_2

doubling run.

The enhancement of the interannual variability of the SST_{MDR} in boreal early summer due to CO_2 doubling could lead to the enhanced year-to-year variations of Atlantic Hurricane count (Table 2) and drought (or flood) in the South American and Sahel region (Fig. 6c), which might be a factor of severe damage in the surrounding contiries. Therefore, we should pay more attention to this enhancement of the interannual variability of the SST_{MDR} in a warmer climate, although most previous work has mainly focused on the future climate change of the annual mean SST and relatively less attention has been paid to response of the interannual variations.

The ultimate cause for the response to CO_2 doubling of the interannual modulation of the meridional migration of the ITCZ and the WES feedback is still open to debate. We showed that the effectiveness of the WES feedback in early boreal summer is stronger in the CO_2 doubling run relative to the Control run. The difference in wind speed anomalies between the CO_2 doubling and the Control run is important for the interannual SST variations in the northern tropical Atlantic. Also, the coupling between the SST variations and the wind speed variations is stronger in the CO_2 doubling run during boreal summer. Since the WES feedback depends on the mean state circulation (e.g. Vimont et al. 2009) and the cross-equatorial SST gradient (e.g. Xie and Carton 2004), the long-lasting interannual WES feedback in a warmer climate may be related to the annual mean changes of the wind and the SST field. As shown in Fig. 2, we found that the weak trade winds in

the tropical Atlantic and the strong warming of the northern tropical Atlantic SST due to CO_2 doubling. The enhancement of the cross-ITCZ meridional SST gradient in boreal spring-summer leads to the northward migraion of the ITCZ. Those responses of the mean SST, wind, and precipitation to CO_2 doubling seem to be coupled via a positive WES feedback. This hemispheric asymmetric response of the mean state associated with the WES feedback due to the global warming is also shown in other climate models (Xie et al. 2011). This hemispheric asymmetric response of the mean state in boreal spring-summer might suggest an enhancement in effectiveness of a WES feedback, which may lead to the large year-to-year variations around the annual mean. Further sensitive experiments with a coupled GCM are necessary to understand the mechanism of the change of the WES feedback's effectiveness due to CO_2 doubling. Also, the difference in the wind anomalies over the MDR between the CO_2 doubling and the Control run seems to be significantly related to the zonal wind in the eastern Pacific in 5°-10°N (figure not shown). Previous work showed that strong ENSO events in the Pacific can partly lead to the warm SST in the northern tropical Atlantic (see Xie and Carton 2004 for a recent review on the Tropical Atlantic Variability). Results from GFDL-CM2.1 and CM2.5 suggest that the amplitude of ENSO events is slightly stronger in the CO_2 doubling experiment than in the Control run (A. Wittenberg, pers. comm.; Delworth et al. 2012). Also, Czaja (2004) suggested that the seasonal dependence of the interannual variability in the northern tropical Atlantic is reflected not only by Atlantic local air-sea coupling, but also by the remote forcing of the

North Atlantic Oscillation and ENSO. Biasutti and Sobel (2009) discussed the idea that the delayed phase of the West African monsoon in a warmer climate is due to sea ice loss at high-latitudes. For the Atlantic Hurricane prediction, not only SST_{MDR}, but also the global tropical mean SST is important (Zhao et al. 2009; Zhao et al. 2010; Vecchi et al. 2011). Exploring the relation between the Northern Tropical Atlantic and other basins will be the focus of further work.

Finally, we discuss robustness of our main new result: the enhancement of the interannual variation of SST_{MDR} in boreal early summer due to CO_2 doubling. Breugem et al. (2007) show that the Atlantic Meridional Mode weakens in the CO_2 doubling run with an atmospheric model coupled to a mixed-layer ocean model. CM2.5 shows an increase in the SST_{MDR} interannual variability, which might suggest a stronger AMM due to CO_2 doubling. However, CM2.5 (also CM2.1 and other CMIP3 models) shows the warm SST biases in the eastern equatorial and southern tropical Atlantic, although the climatology of tropical North Atlantic variability in the high-resolution coupled model used here is substantially improved relative to previous generation models (Doi et al. 2012). It may be difficult to realistically identify the robust response of the Tropical Atlantic Variability to CO_2 doubling in coupled GCMs, since almost all CMIP3 climate models had serious biases in the annual mean tropical Atlantic (Ricther and Xie 2008) and the seasonal phase-locking of the interannual variations of the northern tropical Atlantic SST (figure not shown). Further intercomparisons among coupled climate models with reduced tropical Atlantic biases will

help to clarify the robustness of our results, which have new important implications and make solid progress for tropical Atlantic climate modeling.

Acknowledgments

We thank to Drs. Andrew Wittenberg, Ming Zhao, Rym Msadek, and Ian Lloyd for helpful comments and suggestions. We are grateful to the GFDL-CM2.5 modeling team for their assistance with model infrastructure support and data processing.

References

Breugem, W.-P., W. Hazeleger, and R. J. Haarsma, 2007: Mechanism of Northern Tropical Atlantic Variability and response to CO_2 doubling. *J Climate,* **20,** 2691-2705.

Carton, J. A., X. Cao, B. S. Giese, and A. M. da Silva, 1996: Decadal and interannual SST variability in the tropical Atlantic Ocean. *J. Phys. Oceanogr.*, **26**, 1165-1175.

Chang, P., L. Ji, and H. Li, 1997: A decadal climate variation in the tropical Atlantic ocean from thermodynamic air-sea interactions. *Natue,* **385,** 516-518.

Chen, J H., and Shian-Jiann Lin, 2012: The remarkable predictability of inter-annual variability of Atlantic hurricanes during the past decade. *Geophys. Res. Lett.*, **38**, L11804, DOI:10.1029/2011GL047629.

Chiang, J. C. H., M. Biasutti, and D. S. Battisti, 2003: Sensitivity of the Atlantic ITCZ to Last Glacial Maximum boundary conditions. *Paleoceanography*, **18**, doi:10.1029/2003PA000916.

Cook, K., 2008: The mysteries of Sahel droughts. *Nature Geoscien*ce, **1**, 647-648.

Czaja, A., 2004: Why is North Tropical Atlantic SST variability stronger in boreal spring? *J. Climate*, **17,** 3017-3025.

Delworth, T. L., and Coauthors, 2006: GFDLs CM2 global coupled climate models. Part Ⅰ: Formulation and simulation characteristics. *J. Climate*, **19,** 643-674.

Delworth, T. L., and Coauthors, 2012: Simulated climate and climate change in the

GFDL-CM2.5 high-resolution coupled climate model. *J. Climate*, **25,** 2755-2781

Ding, H., N. S. Keenlyside, M. Latif, 2011: Impact of the equatorial Atlantic on the El Niño Southern Oscillation. *Climate Dyn.,* DOI: 10.1007/s00382-011-1097-y.

Doi, T., G. A. Vecchi, A. J. Rosati, and T. L. Delworth, 2012: Tropical Atlantic biases in the mean state, seasonal cycle, and interannual variations for a coarse and a high resolution coupled climate model, *J. Climate,* **25,** 5494-5511

Enfield, D. B., and D. A. Mayer, 1997: Tropical Atlantic sea surface temperature variability and its relation to El Niño-Southern Oscillation, *J. Geophys. Res.*, **102,** 929-945.

Emanuel, K., 2005: Increasing destructiveness of tropical cyclones over the past 30 years. *Nature*, **436,** 686-688.

Farneti, R., T. L. Delworth, A. J. Rosati, S. M. Griffies, F. Zeng, 2010: The role of mesoscale eddies in the rectification of the Southern Ocean response to climate change. *J. Phys. Oceanogr.*, **40**, 1539–1557.

Gnanadesikan, A., and Coauthors, 2006: GFDL's CM2 global coupled climate models. Part II: The baseline ocean simulation. *J. Climate*, **19,** 675–697.

Griffies, S. M., 2010: Elements of MOM4p1. *GFDL OCEAN GROUP TECHNICAL REPORT NO. 6*, p444.

Griffies, S. M., and coauthors, 2012: GFDL's CM3 Coupled climate model: characteristics of the ocean and sea ice simulations. *Journal of Climate, in press*.

Hagos, S. M., and K. H. Cook, 2009: Development of a coupled regional model and its

application to the study of interactions between the West African monsoon and the eastern tropical Atlantic Ocean. *J. Climate,* **22,** 2591-2604.

Held, I. M., T. L. Delworth, J. Lu, K. L. Findell, and T. R. Knutson, 2005: Simulation of Sahel drought in the 20th and 21st centuries. *Proc. Natl. Acad. Sci.*, **102,** 17891–17896.

Knutson, T. R., coauthors, 2010: Tropical cyclones and climate change. *Nature Geoscience* **3**, 157-163.

Kossin, J. P., and D. J. Vimont, 2007: A more general framework for understanding Atlantic hurricane variability and trends. *Bull. Amer. Meteor. Soc.*, **88**, 1767–1781.

Kucharski, F., A. Bracco, J. Y. Yoo, and F. Molteni, 2008: Atlantic forced component of the Indian monsoon interannual variability. *Geophys. Res. Lett.*, **35**, doi:10.1029/2007GL033037.

Kucharski, F., I.-S. Kang, R. Farneti, and L. Feudale, 2011: Tropical Pacific response to 20th century Atlantic warming, *Geophys. Res. Lett.*, **38**, doi:10.1029/2010GL046248.

Kushnir, Y., W. A. Robinson, P. Chang, and A. W. Robertson, 2006: The physical basis for predicting Atlantic sector seasonal to interannual climate variability. *J. Climate*, **19,** 5949-5970.

Levitus, S., 1982: Climatological Atlas of the World Ocean, NOAA Professional Paper 13, U.S. Department of Commerce.

Lin, S-J., 2004: A "vertically Lagrangian" finite-volume dynamical core for global models. *Mon. Wea. Rev.,* **132,** 2293-2307.

Lu, R., B. Dong, and H. Ding (2006), Impact of the Atlantic Multidecadal Oscillation on the Asian summer monsoon, *Geophys. Res. Lett.*, **33**, doi:10.1029/2006GL027655.

Mahajan, S., R. Saravanan, P. Chang, 2010: Free and forced variability of tropical Atlantic: Role of the Wind-Evaporation-Sea surface temperature (WES) feedback. *J. Climate*, **23**, 5958-5977.

Meehl, G. A., and coauthors, 2007: The WCRP CMIP3 multimodel dataset - A new era in climate change research. *Bull. Amer. Meteor. Soc.,* **88,** 1383-1394.

Milly, P. C. D., S. L. Malyshev, E. Shevliakova, K. A. Dunne, K. L. Findell, K. Eng, T. Gleeson, Z. Liang, P. Phillips, R. J. Stouffer, and S. Swenson. Enhanced Representation of Land Physics for Earth-System Modeling. *in preparation*.

Putman, W M., and Shian-Jiann Lin, 2007: Finite-volume transport on various cubed-sphere grids**.** *J. Computational Phys.*, **227**, 55-78.

Rayner, N. A., and Coauthors, 2003: Global analyses of sea surface temperature, sea ice, and night marine air temperature since the late nineteenth century. *J. Geophys. Res.,* **108**, doi:10.1029/2002JD002670.

Richter, I., and S. P. Xie, 2008: On the origin of equatorial Atlantic biases in coupled general circulation models. *Climate Dyn.,* **31**, 587-598.

Shevliakova E, Pacala S, Malyshev S, Hurtt G, Milly P, Caspersen J, Sentman L, Fisk J, Wirth C, Crevoisier C. 2009. Carbon cycling under 300 years of land use change: Importance of the secondary vegetation sink. *Global Biogeochemical Cycles* **23**,

doi:10.1029/2007GB003176.

Smith, T. M., R. W. Reynolds, T. C. Peterson, J. Lawrimore, 2008: Improvements to NOAA's Historical Merged Land–Ocean Surface Temperature Analysis (1880–2006). *J. Climate*, **21,** 2283-2296.

Stouffer R. J., and Coauthors, 2006: GFDL's CM2 global coupled climate models. Part IV: Idealized climate response. *J. Climate,* **19,** 723–740.

Swanson K. L., 2008: Nonlocality of Atlantic tropical cyclone intensities. *Geochem. Geophys. Geosys.* **9,** Q04V01, doi:10.1029/2007GC001844.

Stouffer R. J., and Coauthors, 2006: GFDL's CM2 global coupled climate models. Part IV: Idealized climate response. *J. Climate,* **19,** 723–740.

Sutton R. T., and D. L. R. Hodson, 2005: Atlantic Ocean forcing of North American and European summer climate. *Scinece*, **309**, 115-118.

Sutton R. T., and D. L. R. Hodson, 2007: Climate response to basin-scale warming and cooling of the North Atlantic Ocean. *J. Climate*, **20**, 891-907.

Vecchi, G. A., K. L. Swanson, B. Soden, 2008: Whither hurricane activity? *Science*, **322**, 687-688,

Vecchi, G. A., M. Zhao, G.Villarini, A. Rosati, I. Held, and R. Gudgel, 2011: Hybrid statistical-dynamical predictions of seasonal Atlantic hurricane activity. *Mon. Wea. Rev.,* **139**, 1070-1082.

Villarini, G., G. A. Vecchi, T. R. Knutson, and J. A. Smith, 2011: Is the recorded increase

in short duration North Atlantic tropical storms spurious?, *J. Geophys. Res.*, **116**, doi:10.1029/2010JD015493.

Villarini, G., G. A. Vecchi, and J. A. Smith, 2012: U.S. Landfalling and North Atlantic Hurricanes: Statistical modeling of their frequencies and ratios, *Mon. Wea. Rev.*, doi:10.1175/MWR-D-11-00063.1.

Vimont, D. J., M. Alexander, and A. Fontaine, 2009: Midlatitude Excitation of Tropical Variability in the Pacific: The Role of Thermodynamic Coupling and Seasonality. *J. Climate,* **22,** 518-534.

Wittenberg, A. T., A. Rosati, N.-C.au, and J. J. Ploshay, 2006: GFDL's CM2 global coupled climate models, Part 3: Tropical Pacific climate and ENSO. *J. Climate,* **19,** 698-722.

Xie, S. P., 1999: A dynamic ocean-atmosphere model of the tropical Atlantic decadal variability. *J. Climate*, **12,** 64-70.

Xie, S. P., and J. A. Carton, 2004: Tropical Atlantic variability: patterns, mechanisms, and impacts. *Earth's Climate: The Ocean-Atmosphere Interaction: From Basin to Global Scales, Geophys. Monogr., Vol. 147, Amer. Geophys. Union*, 121-142.

Xie, S. P., C. Deser, G. A. Vecchi, J. Ma, H. Teng, and A. T. Wittenberg, 2011: Global Warming pattern formation: sea surface temperature and rainfall. *J. Climate*, **23,** 966-986.

Zhang, R., and. T. L. Delworth, 2006: Impact of Atlantic multidecadal oscillations on

India/Sahel rainfall and Atlantic hurricanes. *Geophys. Res. Lett.*, **33**, doi:10.1029/2006GL026267.

Zhao, M, I.M. Held, S.-J. Lin, and G. A. Vecchi, 2009: Simulations of global hurricane climatology, interannual variability, and response to global warming using a 50km resolutions GCM. *J. Climate*, **22,** 6653-6678.

Zhao, M, I.M. Held, and G. A. Vecchi, 2010: Retrospective forecasts of the hurricane season using a global atmospheric model assuming persistence of SST anomalies. *Mon. Wea. Rev.,* **138,** 3858-3868.

Table1

Table 1: Summary for the interannual variations of the SST_{MDR} in CM2.5 for model years 91-140. (a) The peak month is defined as the maximum of the interannual variations of the SST_{MDR}. (b) The standard deviation of the interannual variations of the SST_{MDR} in the peak month (ºC). (c) The number of warm SST_{MDR} years used for the composite analysis defined in the text.

	Control run	CO_2 doubling run
(a) Peak month	March	May
(b) Std. in peak month	0.29	0.32
(c) Num. of warm years	7 years	6 years

Table 2: Summary for Atlantic Hurricane count estimated by Hybrid Statistical-Dynamical Predictions Model of Villarini et al (2011) in model years 91-140. For comparison, we include observational estimates from the HadISST dataset in 1982-2005. (a) Annual mean Atlantic Hurricane count, which is calculated by averaging interannual estimates of Hurricane count. (b) Same as (a), but mean count is calculated by substitute mean SST difference to the model of Villarini et al (2011). The difference between (a) and (b) arises from the non-linearity of the model of Villarini et al (2011). Note that the characteristic of (a) and (b) is very similar. (c) Atlantic Hurricane count anomaly averaged in warm SST_{MDR} years. Increasing (decreasing) is shown by positive (negative) value. A bold text shows a value beyond 90% significance level. Note that the interannual variations of Atlantic Hurricane count increases by about 20% in the CO_2 doubling run even the mean count shows reduction.

	(a) Mean $\frac{\sum_{y=91}^{y=140} f(y)}{50}$	(b) Mean $f(\overline{SST})$	(c) Warm SST_{MDR} years
Observation	6.51	6.36	+0.95
CM2.5-Control	6.56	6.36	**+2.12**
CM2.5-CO_2 doubling	5.88	5.69	**+2.55**
CO_2 doubling run minus Control run	-0.68	-0.67	+0.43 (+20%)

Figure captions

Fig. 1: (a) SST averaged in the Main Developing Region for Atlantic Hurricane (MDR: 80°-20°W, 10°-25°N) from the present-day Control run (blue line) and its CO_2 doubling run (red line) with CM2.5 in model years 1-140 (°C). This paper focuses on model years 91-140. A running mean of eight years is applied.

Fig. 2: (a) Annual mean SST in the Control run averaged in model years 91-140 (°C). MDR is shown by black box. (b) Response to CO_2 doubling of annual mean SST (CO_2 doubling run minus Control run) in model years 91-140 (°C). Note that the change in annual mean SST between CO_2 doubling run and Control run is beyond one standard deviation of interannual variations of annual mean SST in the Control run everywhere in this figure. (c) Same as (a), but for rainfall (mm day^{-1}). Contour interval is 1mm day^{-1}. Red dashed line shows the latitude of the mean Atlantic ITCZ in the Control run. Grey shading denotes that the change in annual mean rainfall between CO_2 doubling run and Control run is beyond one standard deviation of interannual variations of annual mean rainfall in the Control run. (d) Same as (b), but for rainfall. Contour interval is 0.5mm day^{-1}. (e) Same as (a), but for wind stress (N m^{-2}). (f) Same as (b), but for wind stress (N m^{-2}). Contour interval is 0.0025N m^{-2}.

Fig. 3: Mean seasonal variations of SST_{MDR} from the annual mean in the present-day Control (blue line), the CO_2 doubling run (red line), and the HadISST 1960-2009 averaged climatology (grey line) (°C).

Fig. 4: (a) Time series of monthly SST_{MDR} anomalies in the present-day Control (blue line) and the CO_2 doubling run (red line) in model years 91-140 (°C). (b) Probability density function of monthly SST_{MDR} anomaly in model years 91-140 in the present-day Control (blue line) and the CO_2 doubling run (red line) (%).

Fig. 5: (a) Monthly standard deviation of the interannual variation of the SST_{MDR} for the

present-day Control (thick blue line) and the CO_2 doubling run (thick red line) in model years 91-140 (°C). The thin blue lines show the four other 50-years mean standard deviations in the Control run. A running mean of three months is applied. (b) Same as (a), but for observation averaged in three periods of 1881-2009, 1960-2009, and 1881-1930 in ERSSTv3 (black) and HadISST (grey).

Fig.6: (a) Difference in composite anomalies for SST between the recent 50 years (1960-2009) minus the early 50 years (1881-1930) from the HadISST data for May-July in warm SST_{MDR} years (°C). Contour interval is 0.1°C. Grey shading denotes anomalies above 90% significance level. MDR is shown by solid box. (b) Similar to (a), but response to CO_2 doubling of composite anomalies for SST in the CO_2 doubling run minus the Control run. (c) Same as (b), but for rainfall in the CO_2 doubling run minus the Control run (mm day^{-1}). Contour interval is 1mm day^{-1}.

Fig. 7: Diagnostic bulk mixed-layer heat balance anomaly over the MDR (10^{-7} K s^{-1}). Rate of change of SST_{MDR} is determined by $\frac{Q - q_{sw}}{\rho C_p H_{mix}}$:sea surface enthalpy flux contribution and ocean dynamical contribution by Eq. (1) in the text. A running mean of three months is applied. (a) Warm SST_{MDR} years composite in the Control run of CM2.5. (b) Same as (a), but for the CO_2 doubling run. (c) Same as (a), but for difference between the CO_2 doubling run and the Control run. (d) Warm SST_{MDR} years composite in the Control run for surface enthalpy flux anomaly over the MDR (W m^{-2}). *Q*: net surface enthalpy flux anomaly "Net. Hflx" is determined by shortwave radiation "SW", wind-induced latent heat "LH(wind)", moisture-induced latent heat "LH(moisture)", longwave radiation 'LW', and sensible heat "SH" fluxs. A running mean of three months is applied. (e) Same as (d), but for the CO_2 doubling run. (f) Same as (d), but for difference between the CO_2 doubling run and the Control run.

Fig. 8: (a) Response to CO_2 doubling of composite anomalies for the wind-induced latent

heat flux in the CO_2 doubling run minus the Control run, $\left.\frac{\partial Q_{LH}}{\partial W}\right|_{CO_2} W'_{CO_2} - \left.\frac{\partial Q_{LH}}{\partial W}\right|_{CTL} W'_{CTL}$ in the text, for April-June in warm SST_{MDR} years (W m^{-2}). Positive values shows warming ocean. Contour interval is 5W m^{-2}. Color shading denotes anomalies above 90% significance level. MDR is shown by solid box. (b) Same as (a), but for wind stress (N m^{-2}; vector). Red (blue) shading denotes weak (strong) anomalies above 90% significance.

Figures

Fig.1

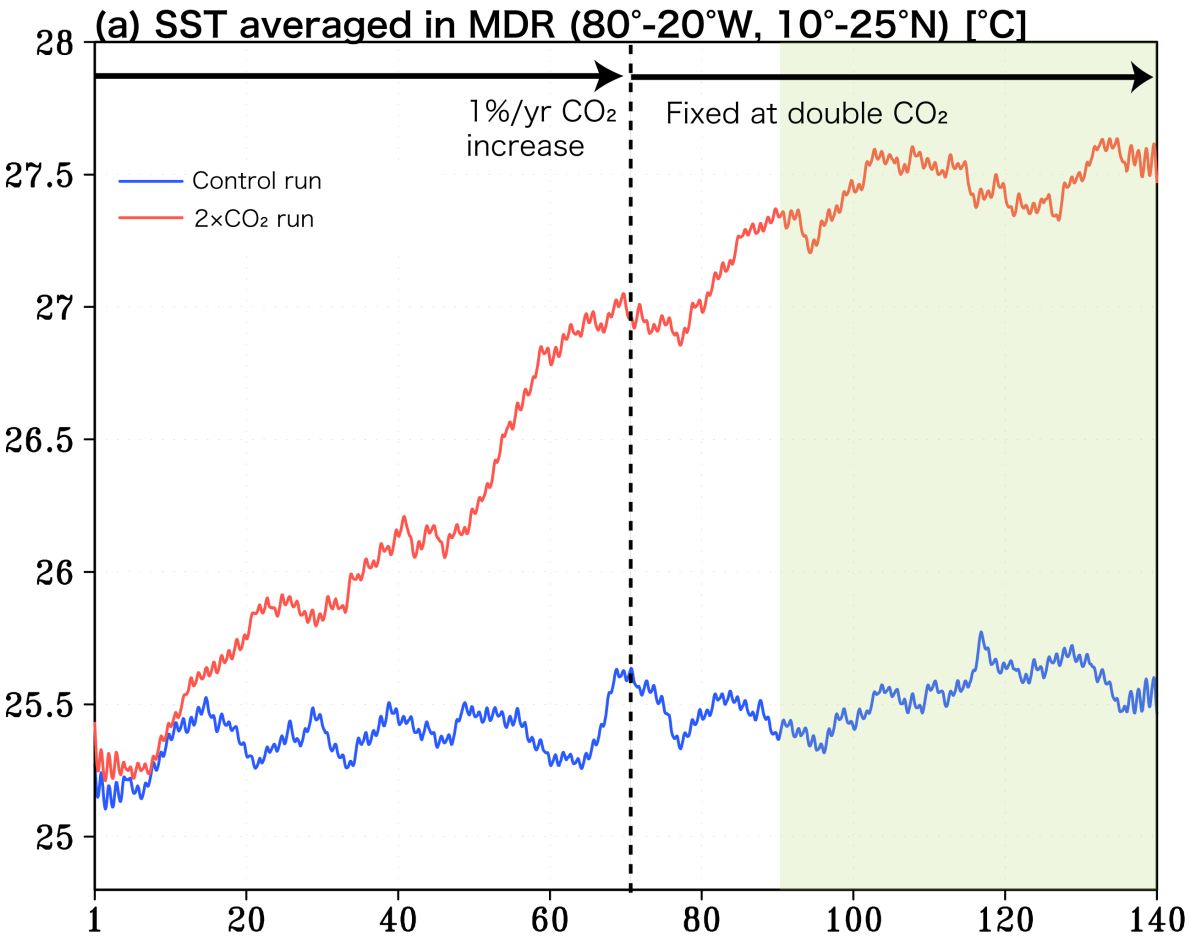

Fig. 1: (a) SST averaged in the Main Developing Region for Atlantic Hurricane (MDR: 80°-20°W, 10°-25°N) from the present-day Control run (blue line) and its CO_2 doubling run (red line) with CM2.5 in model years 1-140 (°C). This paper focuses on model years 91-140. A running mean of eight years is applied.

1 Fig.2

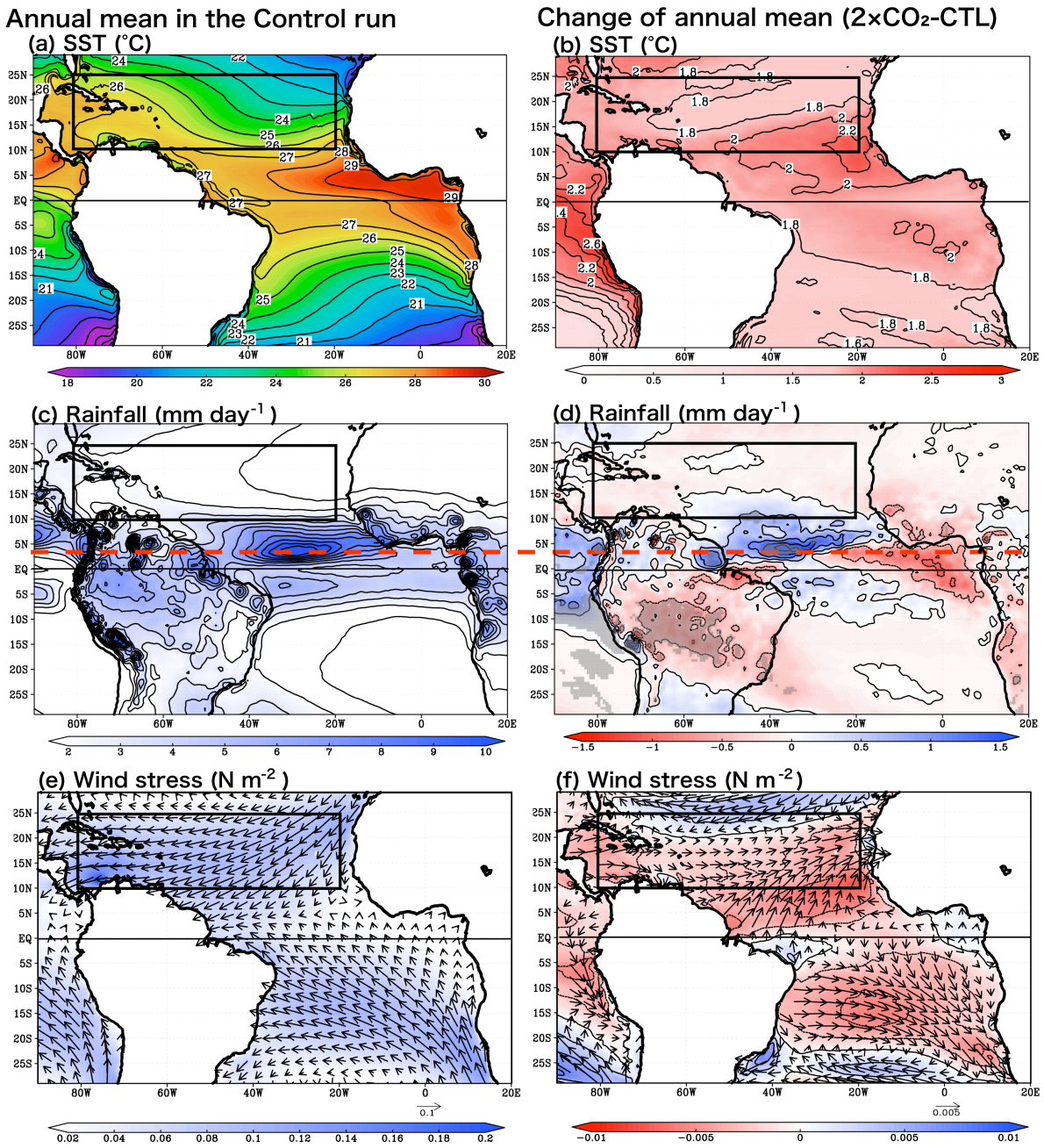

2

3 Fig. 2: (a) Annual mean SST in the Control run averaged in model years 91-140 (°C). MDR
4 is shown by black box. (b) Response to CO_2 doubling of annual mean SST (CO_2 doubling
5 run minus Control run) in model years 91-140 (°C). Note that the change in annual mean
6 SST between CO_2 doubling run and Control run is beyond one standard deviation of

interannual variations of annual mean SST in the Control run everywhere in this figure. (c) Same as (a), but for rainfall (mm day^{-1}). Contour interval is 1mm day^{-1}. Red dashed line shows the latitude of the mean Atlantic ITCZ in the Control run. Grey shading denotes that the change in annual mean rainfall between CO_2 doubling run and Control run is beyond one standard deviation of interannual variations of annual mean rainfall in the Control run. (d) Same as (b), but for rainfall. Contour interval is 0.5mm day^{-1}. (e) Same as (a), but for wind stress (N m^{-2}). (f) Same as (b), but for wind stress (N m^{-2}). Contour interval is 0.0025N m^{-2}.

Fig. 3

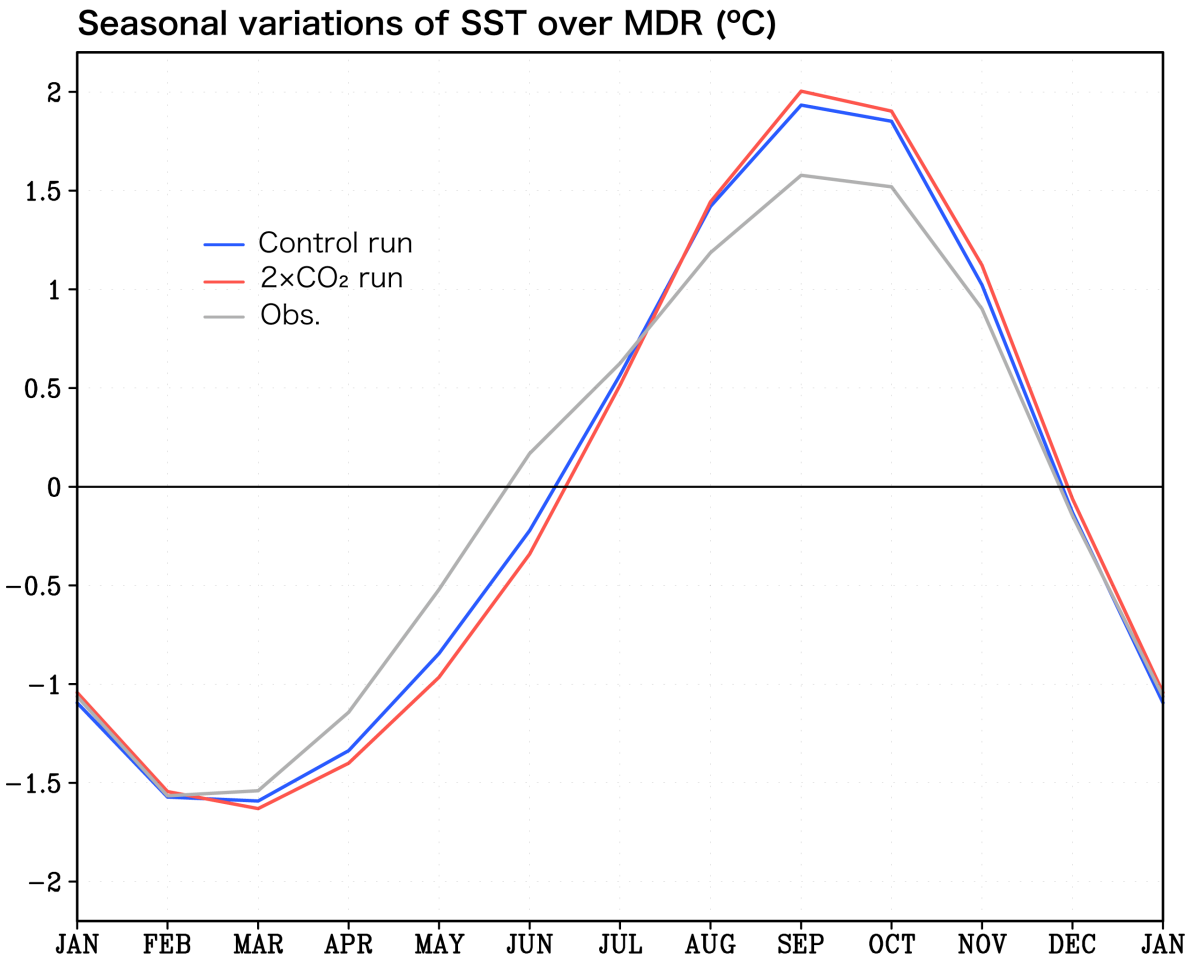

Fig. 3: Mean seasonal variations of SST_{MDR} from the annual mean in the present-day Control (blue line), the CO_2 doubling run (red line), and the HadISST 1960-2009 averaged climatology (grey line) (°C).

Fig. 4

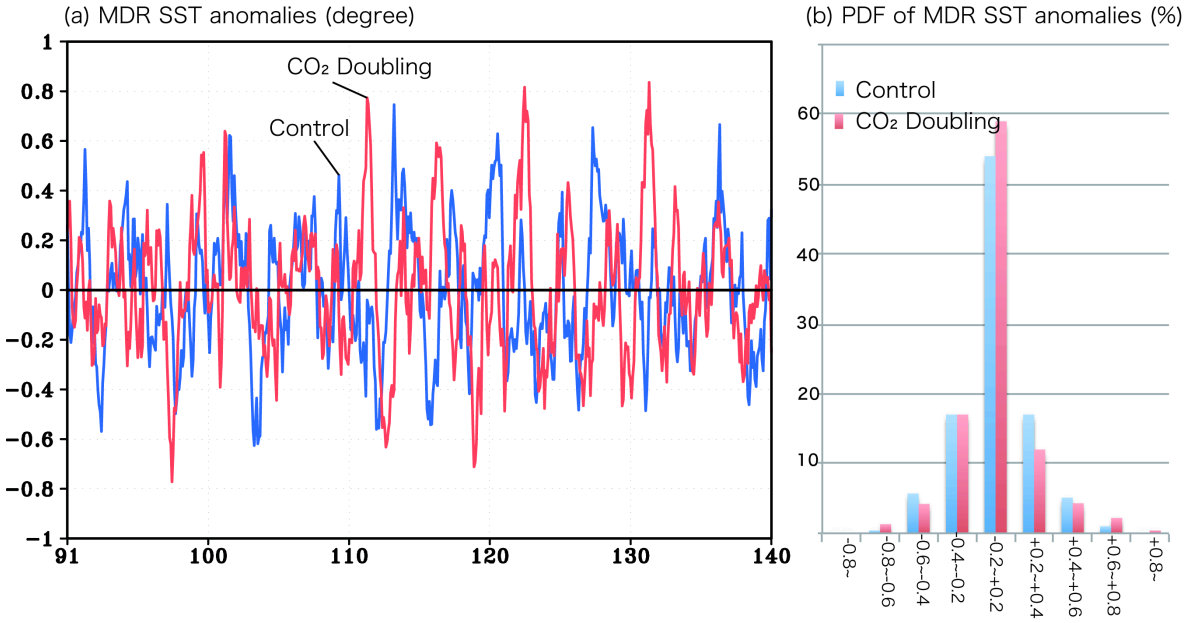

Fig. 4: (a) Time series of monthly SST_{MDR} anomalies in the present-day Control (blue line) and the CO_2 doubling run (red line) in model years 91-140 (°C). (b) Probability density function of monthly SST_{MDR} anomaly in model years 91-140 in the present-day Control (blue line) and the CO_2 doubling run (red line) (%).

1

1 Fig. 5

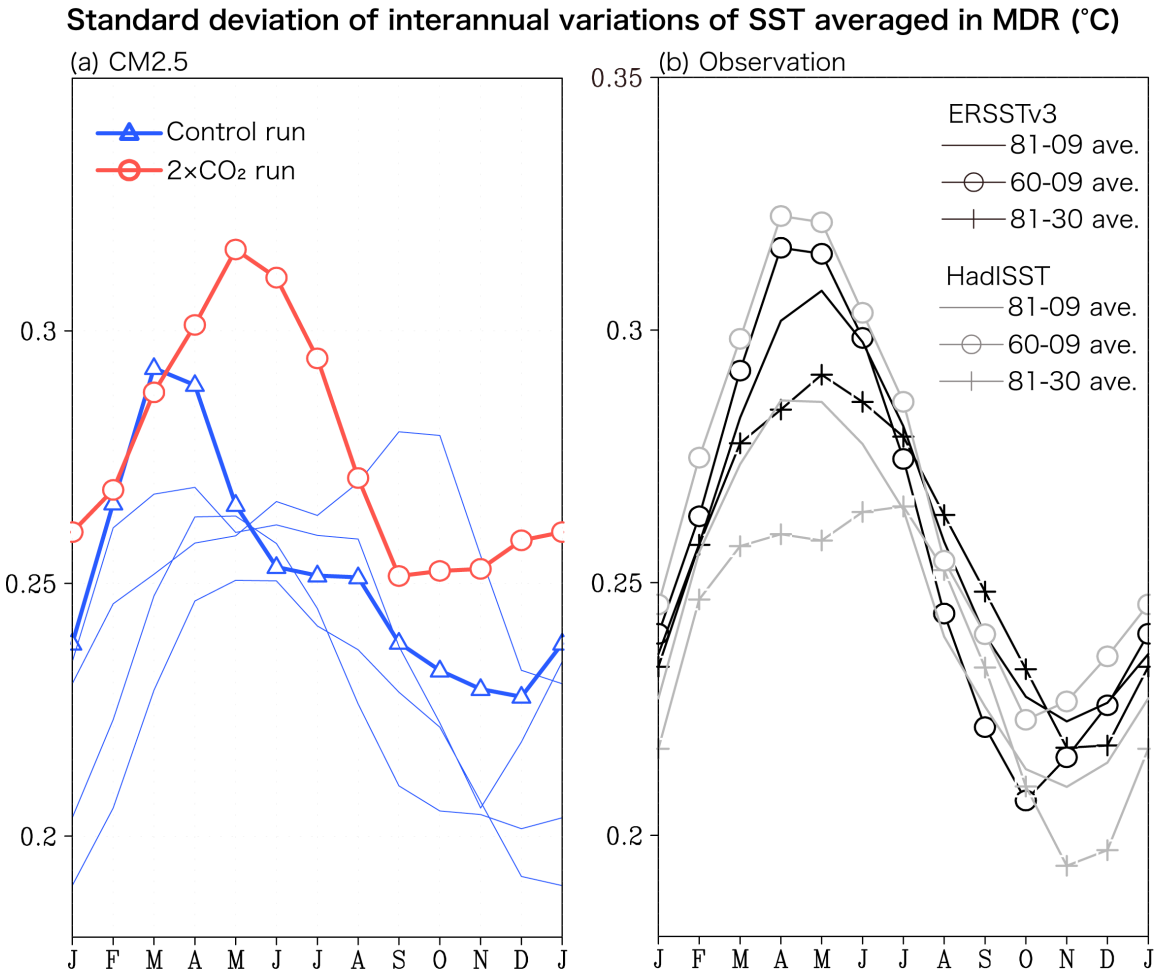

2

3 Fig. 5: (a) Monthly standard deviation of the interannual variation of the SST_{MDR} for the
4 present-day Control (thick blue line) and the CO_2 doubling run (thick red line) in model
5 years 91-140 (°C). The thin blue lines show the four other 50-years mean standard
6 deviations in the Control run. A running mean of three months is applied. (b) Same as (a),
7 but for observation averaged in three periods of 1881-2009, 1960-2009, and 1881-1930 in
8 the ERSSTv3 (black) and HadISST data (grey).

1 Fig.6

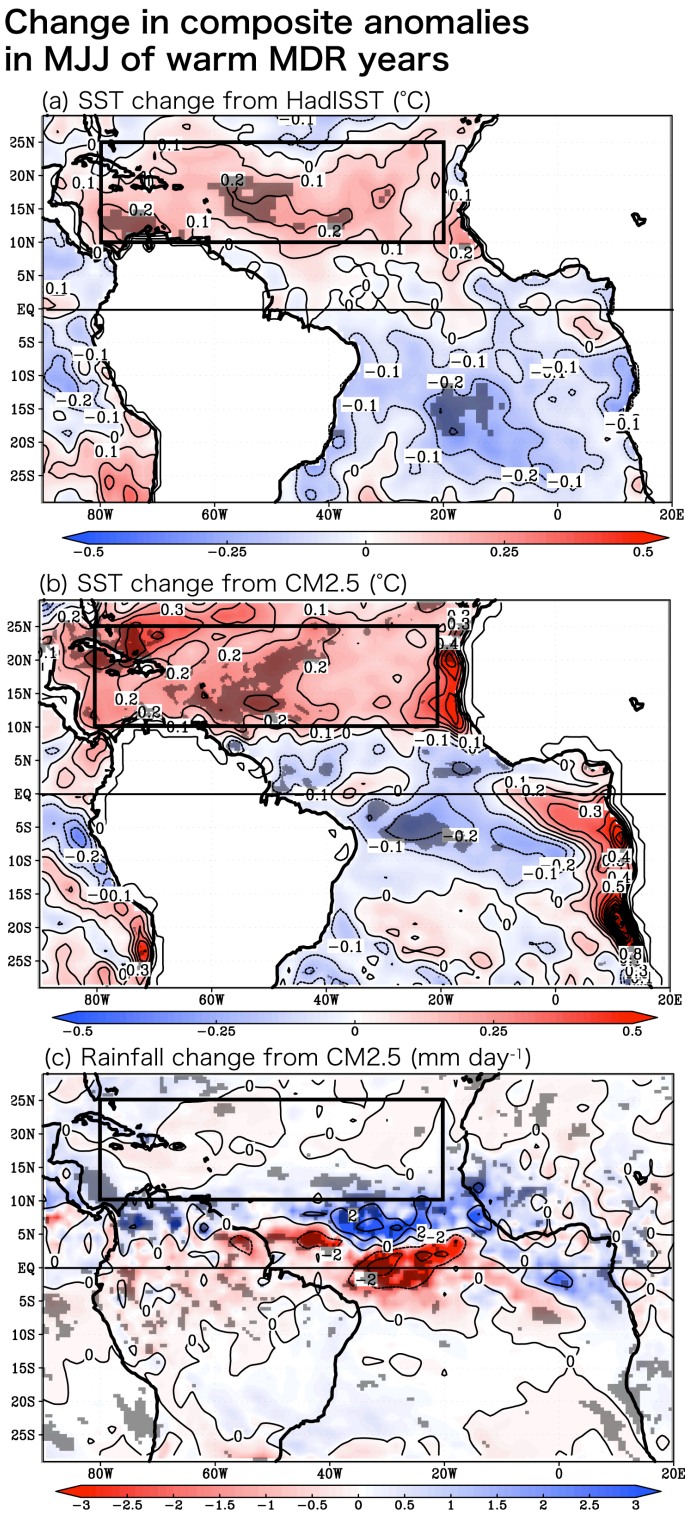
Change in composite anomalies
in MJJ of warm MDR years
(a) SST change from HadISST (°C)
(b) SST change from CM2.5 (°C)
(c) Rainfall change from CM2.5 (mm day⁻¹)
25N
20N
15N
10N
5N
EQ
5S
10S
15S
20S
25S
80W
60W
40W
20W
0
20E
−0.5
−0.25
0
0.25
0.5
−3
−2.5
−2
−1.5
−1
−0.5
0
0.5
1
1.5
2
2.5
3

2

1 Fig.6: (a) Difference in composite anomalies for SST between the recent 50 years
2 (1960-2009) minus the early 50 years (1881-1930) from the HadISST data for May-July in
3 warm SST_{MDR} years (°C). Contour interval is 0.1°C. Grey shading denotes anomalies above
4 90% significance level. MDR is shown by solid box. (b) Similar to (a), but response to CO_2
5 doubling of composite anomalies for SST in the CO_2 doubling run minus the Control run.
6 (c) Same as (b), but for rainfall in the CO_2 doubling run minus the Control run (mm day^{-1}).
7 Contour interval is 1mm day^{-1}.

Fig.7

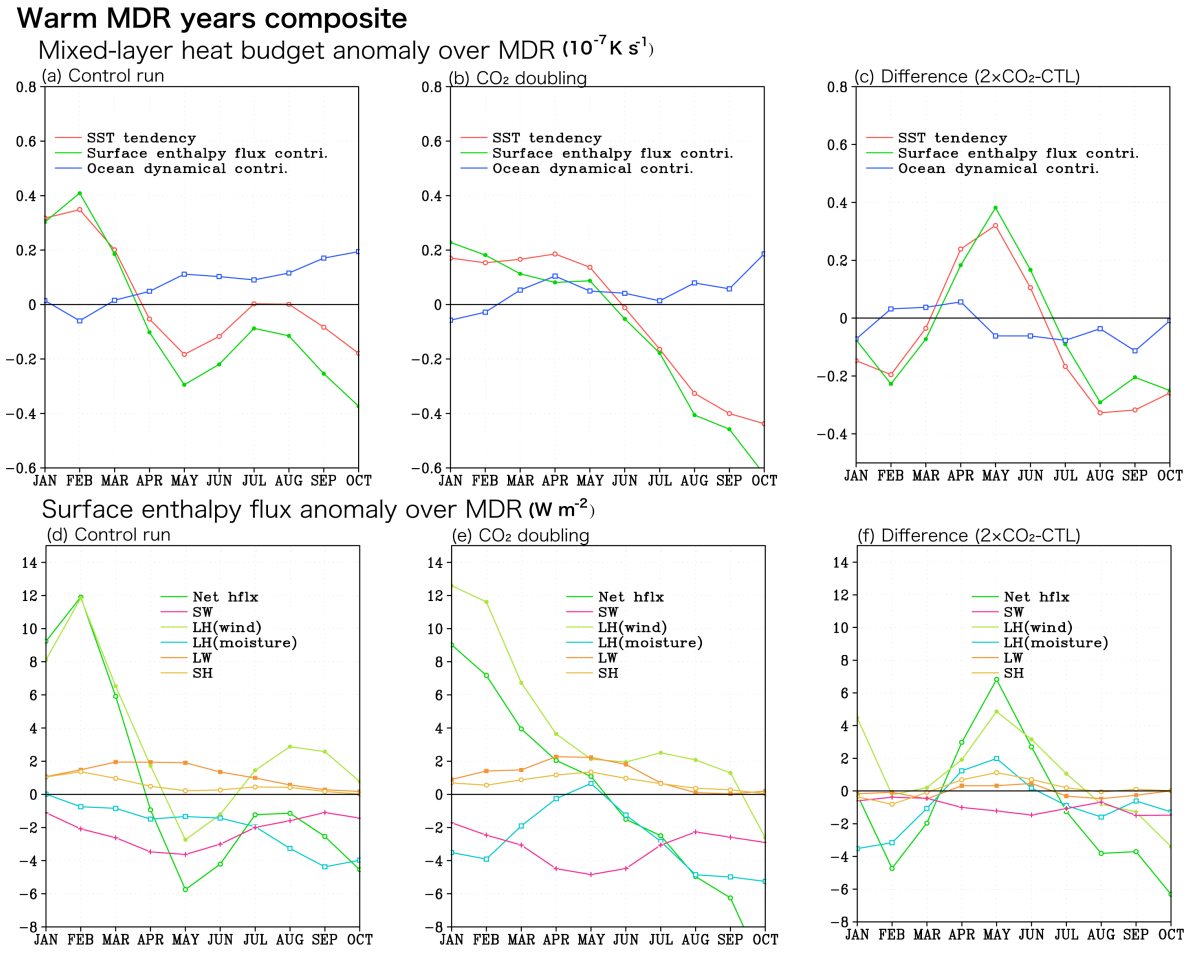

Fig. 7: Diagnostic bulk mixed-layer heat balance anomaly over the MDR (10^{-7} K s^{-1}). Rate of change of SST_{MDR} is determined by $\frac{Q-q_{sw}}{\rho C_p H_{mix}}$:sea surface enthalpy flux contribution and ocean dynamical contribution by Eq. (1) in the text. A running mean of three months is applied. (a) Warm SST_{MDR} years composite in the Control run of CM2.5. (b) Same as (a), but for the CO_2 doubling run. (c) Same as (a), but for difference between the CO_2 doubling run and the Control run. (d) Warm SST_{MDR} years composite in the Control run for surface enthalpy flux anomaly over the MDR (W m^{-2}). Q: net surface enthalpy flux anomaly "Net. Hflx" is determined by shortwave radiation "SW", wind-induced latent heat "LH(wind)", moisture-induced latent heat "LH(moisture)", longwave radiation 'LW', and sensible heat "SH" fluxs. A running mean of three months is applied. (e) Same as (d), but for the

CO_2 doubling run. (f) Same as (d), but for difference between the CO_2 doubling run and the Control run.

Fig.8

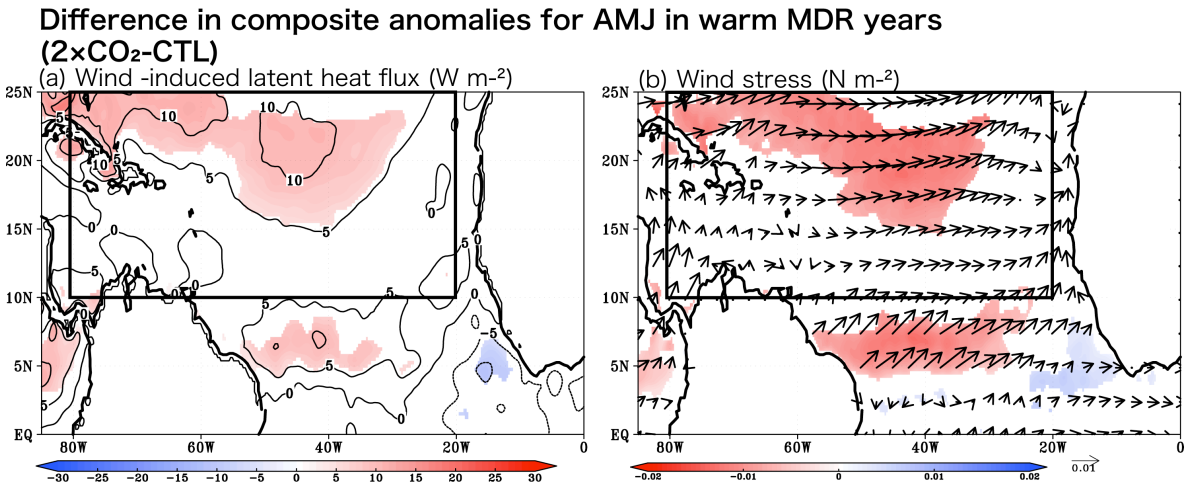

Fig. 8: (a) Response to CO_2 doubling of composite anomalies for the wind-induced latent heat flux in the CO_2 doubling run minus the Control run, $\left.\frac{\partial Q_{LH}}{\partial W}\right|_{CO_2} W'_{CO_2} - \left.\frac{\partial Q_{LH}}{\partial W}\right|_{CTL} W'_{CTL}$ in the text, for April-June in warm SST_{MDR} years (W m^{-2}). Positive values shows warming ocean. Contour interval is 5W m^{-2}. Color shading denotes anomalies above 90% significance level. MDR is shown by solid box. (b) Same as (a), but for wind stress (N m^{-2}; vector). Red (blue) shading denotes weak (strong) anomalies above 90% significance.